Effect of Fe_2O_3 on the transport and magnetic properties of half metallic Fe_3O_4

D. Tripathy and A. O. Adeyeye[a)]
Information Storage Materials Laboratory, Department of Electrical and Computer Engineering, National University of Singapore, Singapore 117576, Singapore

C. B. Boothroyd
Institute of Materials Research and Engineering, 3, Research Link, Singapore 117602, Singapore

(Presented on 1 November 2005; published online 21 April 2006)

We present a systematic study of the transport and magnetic properties of half metallic Fe_3O_4 films grown on Si (100) substrates with a Fe_2O_3 buffer layer using electron beam deposition technique. Transmission electron microscope images show the presence of small grains that are well separated by grain boundaries in our polycrystalline films. We observed that the Verwey transition does not appear for our Fe_3O_4 films and tunneling of spin polarized electrons across grain boundaries dominates the transport properties of the films. Magnetic measurements show a reduced magnetization in our films which does not saturate even at high fields. Coercivity of the films increases with decreasing temperature, suggesting the existence of additional anisotropy at low temperatures. Magnetoresistance curves show linear behavior at high fields which may be attributed to second order tunneling through intermediate states in the grain boundaries. At lower fields, the magnetoresistance behavior is governed by direct tunneling. © *2006 American Institute of Physics*.
[DOI: 10.1063/1.2170981]

One of the major steps in developing next generation spintronic devices is the synthesis of magnetic materials with high spin polarization, high electronic conductivity, and high Curie temperature. Half metallic materials having 100% spin polarization at the Fermi level are very attractive for spintronic devices such as magnetic random access memory and magnetic sensors since the magnetoresistance (MR) effect depends on the spin polarization of the materials used.[1] Half metallicity has been predicted for several materials such as CrO_2,[2] $(Co_{1-x}Fe_x)S_2$,[3] NiMnSb,[4] Sr_2FeMoO_6,[5] and $La_{0.7}Sr_{0.3}MnO_3$.[6] An impediment to using any of these half metals in practical devices is their relatively low Curie temperature. Recently, magnetite (Fe_3O_4) has attracted much interest due to its fully spin polarized half metallic character, relatively high electronic conductivity at room temperature, and a high Curie temperature of 850 K. These characteristics can be utilized in the development of tunneling magnetoresistance (TMR) based devices that would operate at room temperature with high efficiency.[7]

Several works have focused on characterizing the magnetic and transport properties of different forms of Fe_3O_4 including single crystals, powders, epitaxial, and polycrystalline films. Tang *et al.*[8] have prepared nanocrystalline Fe_3O_4 films using pulsed laser deposition and observed a maximum negative MR of 12% near 120 K in a field of 9 T. Park *et al.*[9] have grown single layer Fe_3O_4 films of various thicknesses by reactive sputtering and attributed the MR in their polycrystalline films to spin dependent tunneling between contiguous grains that is only determined by the relative alignment of the surface magnetization. Recently, Jain *et al.*[10] have investigated the effect of buffer layer on the electronic properties of Fe_3O_4 grown using electron beam deposition and observed that the Verwey transition temperature, current-voltage characteristics, and growth mechanism of the films is strongly dependent on the buffer layer material used.

In this work, we have investigated the temperature dependent magnetic and transport properties of 40 nm thick Fe_3O_4 films deposited with a 20 nm Fe_2O_3 buffer layer on Si (100) substrates at room temperature using the electron beam deposition technique.

The films were deposited on Si (100) substrates using electron beam deposition from Fe_2O_3 and Fe_3O_4 pellets, respectively. The base pressure of the chamber was better than 3×10^{-7} Torr before deposition while substrate temperature was maintained at 35 °C. We deposited 40 nm thick Fe_3O_4 films on a 20 nm thick Fe_2O_3 buffer layer. The deposition rates for Fe_3O_4 and Fe_2O_3 were 0.3 and 0.1 Å/s, respectively. Phase identification and crystal structures of the films were examined by conventional θ-2θ x-ray diffraction scans using a Cu K_α radiation and transmission electron microscopy (TEM). We observed that highly crystalline Fe_3O_4 with a preferred $\langle 440\rangle$ orientation was obtained. Magnetic properties of the Fe_3O_4 films were characterized using the vibrating sample magnetometer. Electrical contacts to the films were made using standard optical lithography, metallization of 200 nm Al, followed by lift off in acetone. A standard four-probe configuration was used in all transport measurements at various temperatures.

Figure 1 shows the bright field TEM image and selected area diffraction (SAED) pattern for 40 nm of Fe_3O_4 deposited on 20 nm of Fe_2O_3 buffer layer. We observed that the film consists of nearly uniform grains of average size ~8 nm that are randomly distributed and well separated by grain

[a)]Author to whom correspondence should be addressed; electronic mail: eleaao@nus.edu.sg

 © 2006 American Institute of Physics

Downloaded 12 Jul 2006 to 202.6.242.69. Redistribution subject to AIP license or copyright, see http://jap.aip.org/jap/copyright.jsp

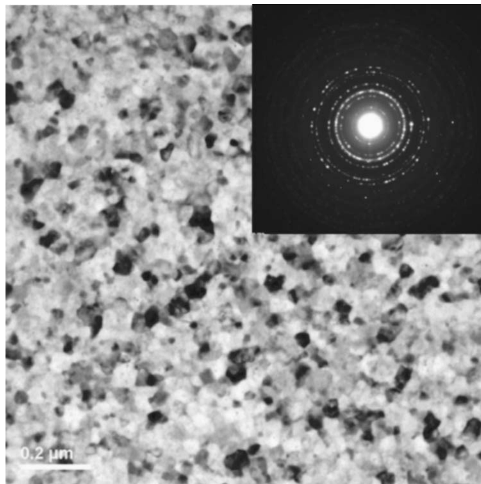

FIG. 1. Bright field TEM image of for 40 nm of Fe_3O_4 deposited on 20 nm of Fe_2O_3 buffer layer. (Inset) SAED pattern.

boundaries. The bright spot in the diffraction pattern comes from the Si (100) substrate while the rings can be indexed to Fe_3O_4, which suggests that the film is polycrystalline. The presence of grain boundaries can alter the magnetic and transport properties of our polycrystalline Fe_3O_4 films significantly from those of bulk Fe_3O_4.

The Verwey transition T_V is a first-order structural phase and metal–insulator transition in which the cubic symmetry of the Fe_3O_4 crystal is broken by a small lattice distortion.[11] Shown in Fig. 2 is the temperature dependence of resistance for 40 nm of Fe_3O_4 deposited on 20 nm of Fe_2O_3 buffer layer. We observed that the Verwey transition, which is usually observed in single crystal samples and relatively thick epitaxial films, does not appear for our Fe_3O_4 film. This disappearance of the Verwey transition in thin films of Fe_3O_4 has been interpreted as being due to several factors such as the small size of ferromagnetic domains and grains[12] and the large density of grain boundaries in the film.[9] From our TEM analysis, we have confirmed the small size of grains and the presence of grain boundaries in the film. Other factors such as residual strain in the Fe_3O_4 film resulting from the Fe_2O_3 buffer layer, small departure from precise Fe_3O_4 stoichiometry,[13,14] lattice mismatch between the Fe_3O_4 film and the substrate, the presence of impurities at the interface

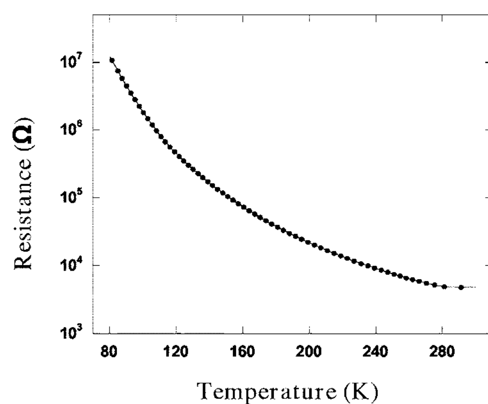

FIG. 2. Resistance as a function of temperature for 40 nm of Fe_3O_4 deposited on 20 nm of Fe_2O_3 buffer layer.

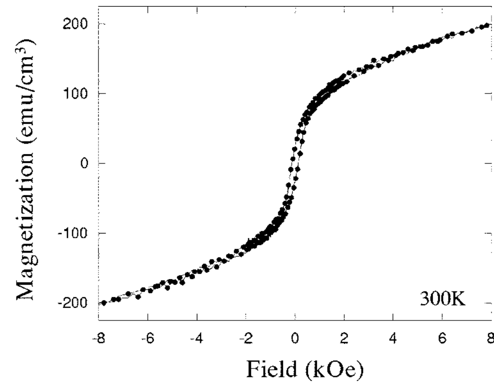

FIG. 3. Magnetization curve for 40 nm of Fe_3O_4 deposited on 20 nm of Fe_2O_3 buffer layer measured at 300 K.

between the Fe_3O_4 film, and the Fe_2O_3 buffer layer and formation of other weakly coupled phases of Fe such as FeO during deposition of the film may also result in the disappearance of the Verwey transition.

We observed that the resistance does not follow either an $\exp[(1/T)]^{1/4}$ law or an $\exp[(1/T)]$ law. The former is observed in the variable range hopping model below T_V, while the latter is applicable to activated conduction through the Coulomb gap above T_V.[15] The disappearance of the Verwey transition suggests that the transport properties of our Fe_3O_4 films are grain boundary controlled. The resistance approximately follows the relation of $R \sim \exp[(1/T)]^{1/2}$. This behavior is expected for a granular system where tunneling occurs through grain boundaries between the grains. A similar dependence has been observed in other granular systems in which grain boundaries act as tunnel barriers for electron tunneling between adjacent grains.[16]

Shown in Fig. 3 is the typical in-plane magnetization curve measured at 300 K for 40 nm of Fe_3O_4 deposited on 20 nm of Fe_2O_3 buffer layer. The coercivity H_C of the film is 178 Oe at room temperature and increases to 350 Oe at 120 K. We observed that the magnetization of the Fe_3O_4 films was unsaturated above 8 kOe at all temperatures, whereas the magnetization is expected to saturate near the anisotropy field H_K of bulk Fe_3O_4, ~310 Oe.[17] Similar anomalous behavior was also observed in nanocrystalline Fe_3O_4 films deposited on Si substrates by pulsed laser deposition,[8] Fe_3O_4 films grown on MgO substrates by dc magnetron reactive sputtering,[18] and Fe_3O_4 films epitaxially grown on MgO substrates.[19] It has been suggested that the anomalous magnetic behavior originates from exchange interactions across antiphase boundaries (APBs).[19] By analogy to the APBs, we suggest that there exists antiferromagnetic (AF) coupling in our polycrystalline films through grain boundaries.

The magnetization value measured at 8 kOe field was ~200 emu/cm^3, which is lower than the typical bulk value of 471 emu/cm^3 for Fe_3O_4 crystal. The existence of strong AF coupling within the grain boundaries causes a reduction in the magnetization of our films. Another possible reason for this low magnetization is the formation of other phases such as wüstite, which is paramagnetic at room temperature and becomes antiferromagnetic at low temperatures. The

Downloaded 12 Jul 2006 to 202.6.242.69. Redistribution subject to AIP license or copyright, see http://jap.aip.org/jap/copyright.jsp

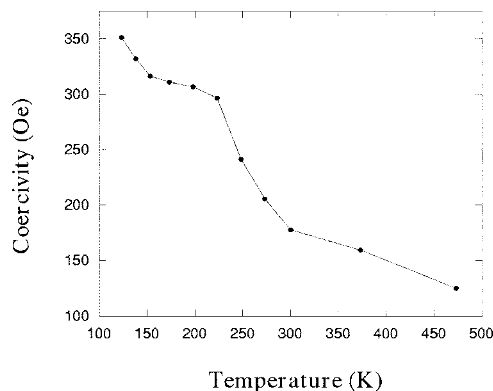

FIG. 4. Coercivity as a function of temperature for 40 nm of Fe_3O_4 deposited on 20 nm of Fe_2O_3 buffer layer.

presence of a Fe_2O_3 buffer below the Fe_3O_4 film may also introduce strain which results in reduction of the overall magnetization. Moreover, the magnetization of Fe_3O_4 thin films is also reduced due to the presence of voids between grains and APBs.[20]

We have performed temperature-dependent magnetization measurements for our Fe_3O_4 films and extracted the coercivity values at various temperatures. Shown in Fig. 4 is the temperature dependence of coercivity for 40 nm of Fe_3O_4 deposited on 20 nm of Fe_2O_3 buffer layer. We can clearly see that the coercivity of our sample increases with decreasing temperature. It should be noted that the mobility of hopping electrons in the Fe_3O_4 drops sharply while the magnetocrystalline anisotropy increases considerably as the lattice structure changes from cubic to monoclinic below the Verwey transition.[21] The increase in coercivity with decreasing temperature suggests the existence of additional anisotropy beyond the bulk value. In Fe_3O_4, the magnetocrystalline anisotropy which originates from the octahedrally coordinated Fe^{2+} ions varies strongly with temperature. This causes a modification of the magnetic domain structure as temperature decreases, and results in an increase in coercivity.

Shown in Fig. 5 are the transverse MR curves for 40 nm of Fe_3O_4 deposited on 20 nm of Fe_2O_3 buffer layer as a function of temperature up to a maximum magnetic field of 4 T. The MR curves show a very weak saturation trend for magnetic fields upto 4 T. At room temperature, a large MR of −7% was observed. MR increases with decreasing temperature and reaches a value of −12.6% at 150 K. We observe that the shape of our MR curves resembles that of intergrain magnetoresistance (IMR). This phenomenon occurs when a network of spin polarized ferromagnetic grains are separated by insulating grain boundaries acting as tunnel barriers. The large degree of spin polarization of half metallic Fe_3O_4 enhances the scale of the IMR effect. We can clearly distinguish between two different regimes in our MR curves; for fields below 1 T, the resistance drops rapidly with applied field while at higher magnetic field, a linear MR is observed. The abrupt low field MR can be qualitatively interpreted within the direct tunneling models applied to ferromagnet/insulator/ferromagnet tunnel junctions.[1,22] The linear behavior of MR in the high field regime maybe interpreted following the model of Lee *et al.*[23] for second order tunneling through an intermediate state in the grain boundary. It is suggested that direct tunneling could be superimposed with second order tunneling, thus resulting in two parallel conduction channels whose conductivities should be linearly added.

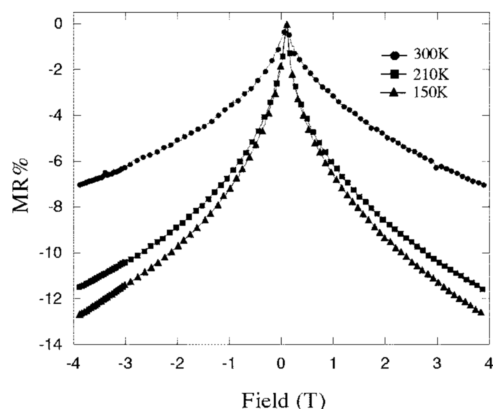

FIG. 5. Magnetoresistance curves as a function of temperature for 40 nm Fe_3O_4 deposited on 20 nm of Fe_2O_3 buffer layer.

This work was supported by National University of Singapore (NUS) Grant No. R263-000-283-112. One of the authors (D.T.) would like to thank NUS for his research scholarship.

[1]M. Julliere, Phys. Lett. **54A**, 225 (1975).
[2]K. Schwarz, J. Phys. F: Met. Phys. **16**, L211 (1986).
[3]I. I. Mazin, Appl. Phys. Lett. **77**, 3000 (2000).
[4]R. A. de Groot, F. M. Mueller, P. G. van Engen, and K. H. J. Buschow, Phys. Rev. Lett. **50**, 2024 (1983).
[5]K. I. Kobayashi, T. Kimura, H. Sawada, K. Terakura, and Y. Tokura, Nature (London) **395**, 677 (1998).
[6]J. H. Parl, E. Vescovo, H. J. Kim, C. Kwon, R. Ramesh, and T. Venkatesan, Nature (London) **392**, 794 (1998).
[7]W. Kim, K. Kawaguchi, N. Koshizaki, M. Sohma, and T. Matsumoto, J. Appl. Phys. **93**, 8032 (2003).
[8]J. Tang, K.Y. Wang, and W. Zhou, J. Appl. Phys. **89**, 7690 (2001).
[9]C. Park, Y. Peng, J. Zhu, D. E. Laughlin, and R. M. White, J. Appl. Phys. **97**, 10C303 (2005).
[10]S. Jain, A. O. Adeyeye, and C. B. Boothroyd, J. Appl. Phys. **97**, 093713 (2005).
[11]E. J. W. Verwey, Nature (London) **144**, 327 (1939).
[12]W. Eerenstein, T. T. M. Palstra, T. Hibma, and S. Celotto, Phys. Rev. B **66**, 20110(R) (2002).
[13]R. Aragon, Phys. Rev. B **46**, 5328 (1992).
[14]G. Rozenberg, G. Hearne, M. Pasternak, P. A. Metcalf, and J. M. Honig, Phys. Rev. B **53**, 6482 (1996).
[15]S. B. Ogale, K. Ghosh, R. P. Sharma, R. L. Greene, R. Ramesh, and T. Venkatesan, Phys. Rev. B **57**, 7823 (1998).
[16]J. Inoue and S. Maekawa, Phys. Rev. B **53**, R11927 (1996).
[17]B. D. Cullity, *Introduction to Magnetic Materials* (Addison-Wesley, Reading, MA, 1972), p. 233.
[18]D. T. Margulies, F. T. Parker, F. E. Spada, R. S. Goldman, J. Li, R. Sinclair, and A. E. Berkowitz, Phys. Rev. B **53**, 9175 (1996).
[19]W. Eerenstein, T. T. M. Palstra, S. S. Saxena, T. Hibma, and S. Celotto, Phys. Rev. B **66**, 201101 (2002).
[20]T. Hibma, F. C. Voogt, L. Niesen, P. A. A. van der Heijden, J. M. de Jonge, J. J. T. M. Donkers, and P. J. vander Zaag, J. Appl. Phys. **85**, 5291 (1999).
[21]J. Yoshida and S. Iida, J. Phys. Soc. Jpn. **47**, 1627 (1979).
[22]S. Zhang, P. M. Levy, A. C. Marley, and S. S. P. Parkin, Phys. Rev. Lett. **79**, 3744 (1997).
[23]S. Lee, H. Y. Hwang, B. I. Shraiman, W. D. Ratcliff II, and S.W. Cheong, Phys. Rev. Lett. **82**, 4508 (1999).

Downloaded 12 Jul 2006 to 202.6.242.69. Redistribution subject to AIP license or copyright, see http://jap.aip.org/jap/copyright.jsp